Tau Identification at DØ *

Cristina Galea, for the DØ Collaboration

Radboud Universiteit Nijmegen/NIKHEF
NL - 6525 ED Nijmegen, The Netherlands

We describe methods to identify τ leptons produced in high energy $p\bar{p}$ collisions ($\sqrt{s}$ = 1.96 GeV) at the Tevatron, using the DØ detector. Different procedures used for discrimination against background particles misidentified as taus are also discussed. Finally, we present some physics results obtained by applying these methods to illustrate their performance.

PACS numbers: 13.38.Dg, 13.85.Qk, 14.70.Hp

1. Introduction

The taus are elusive particles: with a mass of 1.78 GeV and a short lifetime $c\tau$ of 87 μm, no detector in current or near future high energy collision experiments is ever close enough to detect them before they decay. Besides, about half of their energy is carried away invisibly by the tau neutrino, making their detection even harder. So why should one even try?

There are many compelling reasons. The most straightforward one is of course the increased acceptance for channels with leptons: assuming the same efficiency for any lepton identification, this would lead to increase factors of 1.5, 2 and 3 for the single lepton channel, two lepton channel and three lepton channel, respectively. Another reason is the fact that many interesting and yet undiscovered physical processes favor the production of τ leptons compared to most other particles, except maybe the b quarks: the largest coupling of the Higgs boson to leptons is to taus, the minimal SUSY models with large tanβ favor decays to taus as well, and obviously the 3rd

---

* Presented at the conference "Physics at LHC", 3-8 July 2006, Polish Academy of Arts and Sciences, Krakow, Poland

generation of lepto-quarks can only be discovered in the tau channel, if they exist.

The DØ detector is a large general purpose detector for the study of phenomena in high energy $p\bar{p}$ collisions, now in operation at the Fermilab Tevatron Collider. For a complete description of the detector see [1].

2. Tau Triggers

The selection of events containing taus in the final state may start online with triggers specifically designed to favor hadronic tau decays. DØ has a three-tier triggering system and is using both single and di-tau triggers.

The single hadronic tau (τ_h) triggers require a track and a calorimeter tower at Level 1, followed by identification based on a Neural Network (NN) at Level 3 (see section 4 for a discussion on NN). These triggers are used in coincidence with missing transverse energy ($\not{E}_T$) triggers for the $W \to \tau\nu_\tau$ analysis.

The di-tau triggers may be $\mu + \tau_h$, $e + \tau_h$ or $\tau_h + \tau_h$. The analyses with these triggers are at early stages in DØ. For the $Z \to \tau\tau$ and $H \to \tau\tau$ results presented here, single electron and single muon triggers were used.

Due to bandwidth limitations, all τ triggers can add up to a maximum of 2 Hz to tape at instantaneous luminosities of $10^{32}\text{cm}^{-2}\text{s}^{-1}$.

3. The DØ Tau Reconstruction

Within the DØ experiment a tau candidate is a collection of the following objects:

- **Calorimeter Cluster:** reconstructed using the Simple Cone algorithm with cone size $R = 0.5$. A core cone of size $R_{core} = 0.3$ is used for the calculation of isolation variables. The cluster should have $rms < 0.25$, with $rms = \sqrt{\sum_{i=1}^{n}[(\Delta\phi_i)^2 + (\Delta\eta_i)^2]E_{T_i}/E_T}$, where i is the index of the calorimeter tower associated with the τ-cluster.

- **Associated Tracks:** all tracks in a $R = 0.3$ cone around the calorimeter cluster, compatible with a τ decay (invariant mass < 1.8 GeV). At least one track with $p_T > 1.5$ GeV is required.

- **EM sub-clusters:** reconstructed with the Nearest Neighbor algorithm using a seed situated in the third layer of the electromagnetic calorimeter (EM$_3$), where the showers are supposed to reach their maximum. The EM$_3$ also has the highest granularity within the DØ calorimeter. The EM sub-cluster must have an energy E > 800 MeV.

The tau candidates always have a calorimeter cluster. They are then classified into three types, depending on the number of associated tracks and EM sub-clusters they posses:

- **type 1:** only one associated track and no EM sub-clusters

- **type 2:** only one associated track and at least one EM sub-cluster

- **type 3:** at least two associated tracks and ≥ 0 EM sub-clusters

4. Jet background reduction

Due to the high background from jets (more than half of all jets will be misidentified as taus, see Table 1), other selection criteria have to be applied in order to distinguish between jets and taus. Three separate Neural Networks (NN_1, NN_2 and NN_3), one for each τ-type, were trained using taus from Monte Carlo events as signal and jets back-to-back to non-isolated muons from data as background. All NNs presented in this and following sections use a simple back propagation algorithm, with one node for each input variable, one intermediate layer having a number of hidden nodes equal to the number of input nodes, and a single output node.

The input variables used can be classified as follows:

- **isolation variables :** $caliso = (E_T^{\tau} - E_T^{core})/E_T^{core}$,
  $trkiso = \sum p_T^{trk} / \sum p_T^{\tau_{trk}}$, $em12isof = (E^{EM_1} + E^{EM_2})/E^{\tau}$

- **shower shape variables :** rms, EM and $hadronic\ fractions$,
  $profile = E_T^{leading\ 2\ towers}/E_T^{\tau}$, $prf3 = E_T^{leading\ EM\ sub-cluster}/E_T^{EM_3}$

- **calorimeter - track correlation variables :** $E_T^{\tau}/(E_T^{\tau} + \sum p_T^{\tau_{trk}})$,
  $\delta\alpha$ = angle between $\sum \tau_{trk}$ and $\sum EM\ sub\text{-}clusters$

where τ_{trk} (trk) are tracks associated (unassociated) with the tau within the R < 0.5 cone and E^{EM_i} is the energy in ith layer of the EM calorimeter.

Figure 1 shows the distribution of some of these input variables for type 1 tau candidates. One can see that no particular distribution can be used to clearly distinguish between signal and background, but when used together within a NN they can be very effective in making this separation.

The output of a Neural Network should be close to 0 for the background and near 1 for the signal. Figure 2 shows the NN output for background jets and for taus from $Z \rightarrow \tau\tau$ Monte Carlo events for the three τ-types. The distributions are normalized with respect to each other such that the sum over the three τ-types is 1. As shown in Table 1, a cut placed on the NN output variable at 0.9 reduces the jet background by a factor of
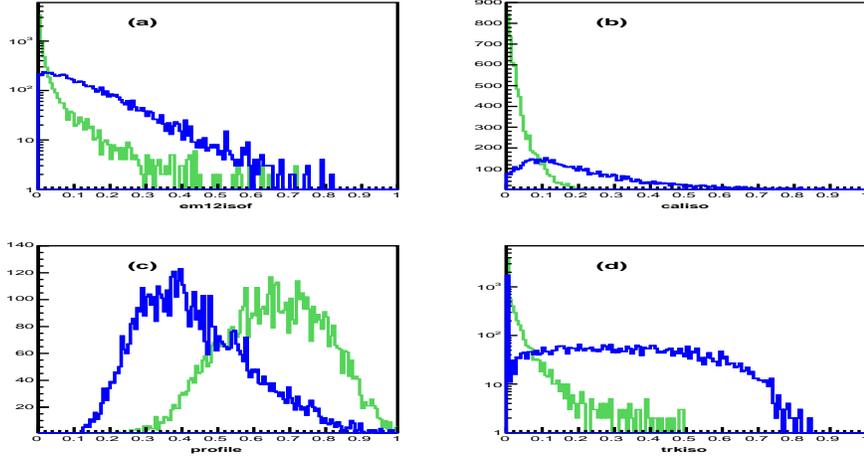
Fig. 1. Some NN input variables distributions for τ-type 1: (a) $em12isof$ (b) $caliso$ (c) $profile$ (d) $trkiso$. The signal distributions are shown in (light) green, while the background ones are shown in (dark) blue.
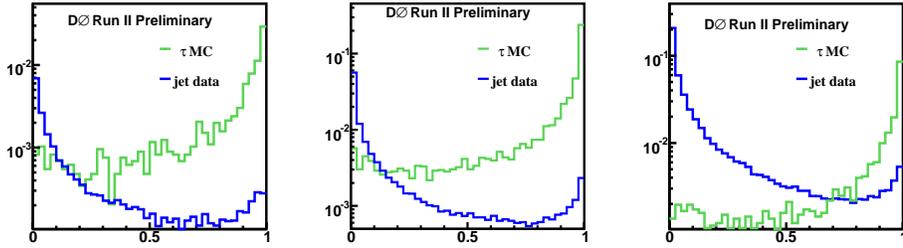

Fig. 2. NN output distributions for type 1 taus (NN$_1$, left), type 2 taus (NN$_2$, middle) and type 3 taus (NN$_3$, right). The signal sample distributions (taus from Monte Carlo) are shown in (light) green, while the background ones (jets back-to-back to non-isolated muons from data) are shown in (dark) blue.

50 to sub-percent levels for all τ-types, while keeping the total efficiency for hadronic taus close to 70 %. The numbers in this table correspond to the tau candidates with transverse energy between 20 and 40 GeV. Note that excluding τ-type 3 would bring a factor of 3 increase in the signal to background ratio, with only a 24 % loss in efficiency.

τ-type	1	2	3	all
jets	2	12	38	52
τ	11	60	24	95
$NN > 0.9$				
jets	0.06	0.24	0.80	1.1
τ	7	44	16	67

Table 1. Efficiencies (%) for tau identification, before and after the NN > 0.9 cut. The numbers include branching ratios and do not include $\tau \to \mu\nu_\mu\nu_\tau$ decays.

5. Electron background reduction

With their often isolated track corresponding to a calorimeter cluster and with most of the showering taking place in the EM layers, the electrons make nice type 2 tau candidates. In fact, they are so similar to the real taus, that a cut placed at 0.9 on the NN_2 output will only reject about 2 % of the electrons. Virtually all electrons will be identified as type 2 taus by all the means we described above. To discriminate against them, a special Neural Network (reffered to by NN_e from now on) was designed using most of the variables described in the previous section, but this time training the NN with electrons from a Monte Carlo sample as background. The results of the NN_e and the output of NN_2 shown in comparisson can be seen in Figure 3. For the transverse energy region of the tau candidate between 20 and 40 GeV, a 0.9 cut on NN_2 would let 98% of the electrons pass, while a 0.5 cut on the NN_e output will reduce the electron background to only 3.4 %, with an efficiency loss for type 2 taus of only 14 % (from 44 % to 38 %).

6. Muon background reduction

Due to the limited coverage of the muon detectors (larger gaps at high η and at the bottom, needed for the calorimeter support and the readout systems) only 80 % of muons faking taus are removed by rejecting tracks reconstructed as muons. About 1.2 % of all muons can still fake tau candidates of types 1 or 2. This can be reduced by a factor of two (from 0.4 % to 0.2 % for type 1, and from 0.8 % to 0.4 % for type 2) by requiring $\mathcal{R}_\mu > 0.4$, where $\mathcal{R}_\mu$ is defined by Equation (1) . This variable exploits the fact that most taus deposit the greatest part of their energy in the inner layers of the calorimeter, while the muons usually do so in the outer layers, namely in the coarse hadronic (CH) section.

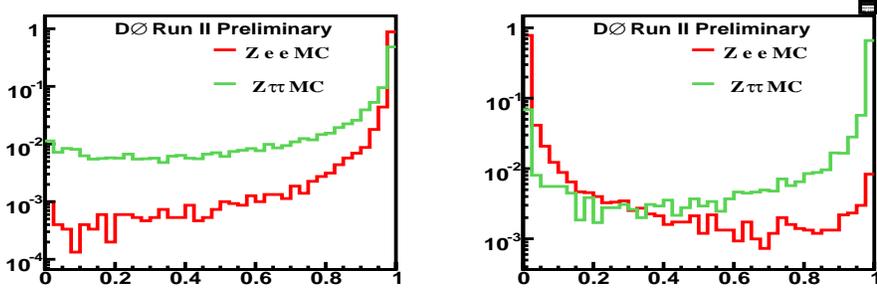$$\mathcal{R}_\mu = \frac{E_T^\tau(1 - f_{CH})}{p_T^{track}} \tag{1}$$

Fig. 3. NN output distributions for τ-type 2: trained on jets as background (NN$_2$, left) and trained on electrons as background (NN$_e$, right). The signal sample distributions (taus from Monte Carlo) are shown in (light) green, while the background ones (electrons from Monte Carlo) are shown in (dark) red.

where E_T^τ is the E_T of the calorimeter cluster, p_T^{track} is the p_T of the associated track and f_{CH} is the fraction of E_T deposited by the tau candidate in the CH layers. Figure 4 shows the effect of the μ identification and $\mathcal{R}_\mu$ cuts on data events containing a muon and a tau candidate matched to a muon.
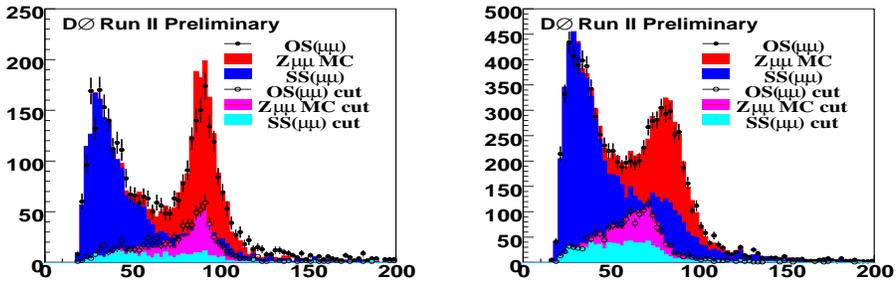

Fig. 4. Invariant mass distributions using a μ and a τ candidate. The dots show data events where the two particles have opposite sign (OS), before (filled) and after (empty) the cuts to remove misidentified muons, for type 1 (left) and type 2 (right) tau candidates. The distributions for same sign (SS) $\mu - \tau$ pairs also shown.

7. Testing the tau identification on data

In order to test the effectiveness of the tau identification and background reduction methods explained in the previous sections, we selected events expected to have a large contribution from $Z \to \tau\tau$. Each event was required to have one and only one isolated muon with $p_T^\mu > 12$ GeV and $|\eta^\mu| < 1.7$, a tau candidate with $E_T > 10$ GeV and $|\eta^\tau| < 2.5$, $\mathcal{R}_\mu > 0.4$ and $|\phi_\mu - \phi_\tau| > 2.7$. The data was selected from a sample of about $\int L dt = 630$ pb^{-1}.
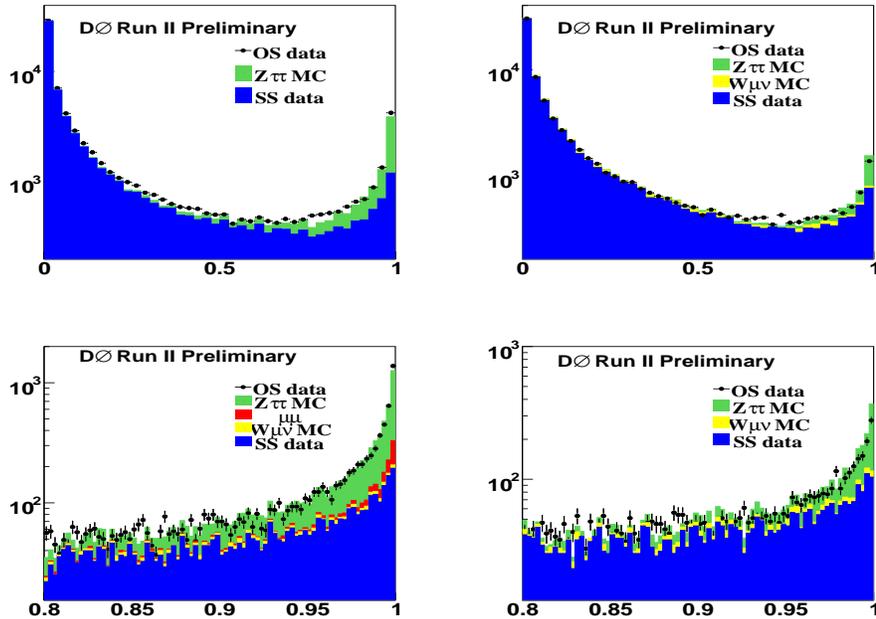
Fig. 5. NN output distributions for the sum of τ-type 1 and τ-type 2 (left) and for τ-type 3 (right).

Figure 5 shows the NN output distributions for events with opposite sign (OS) and same sign (SS) $\mu - \tau$ pairs, before and after the NN > 0.8 cut. The excess of OS events at high NN output values is estimated to come from $Z \to \tau_\mu \tau_{h/e}$ events. This is illustrated by showing the contribution from a $Z \to \tau\tau$ MC sample, normalized to the number of OS events from data after background subtraction. The backgrounds are estimated from data, by selecting same sign $\mu - \tau$ pairs for QCD backgrounds (jets faking taus) or muons misidentified as taus for the $Z \to \mu\mu$ background. High cuts were placed on the muon transverse momentum and missing transverse en-

ergy ($p_T^\mu > 20$ GeV and $\not{E}_T > 20$ GeV) for estimating the $W \to \mu\nu$+jet background. We then rely on Monte Carlo to extrapolate all of these backgrounds into the signal region.

After all cuts have been applied, there are close to 5000 taus above an equivalent amount of background in this sample. Figure 6 shows the invariant mass distributions of the μ - τ pairs after the NN > 0.8 cut.
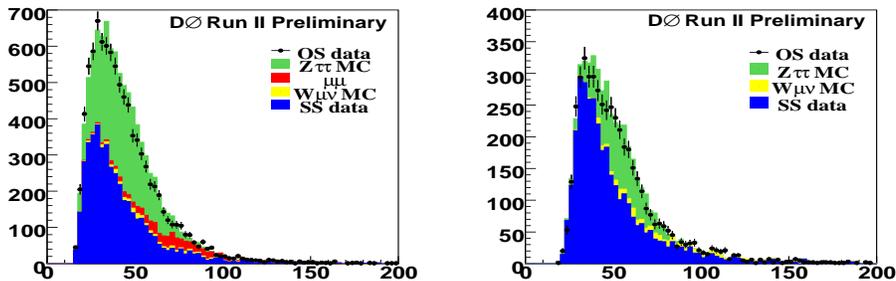

Fig. 6. Invariant mass distributions of the μ and all the tracks associated with the τ-candidate for the sum of τ-type 1 and τ-type 2 (left) and for τ-type 3 (right).

8. Physics results using tau identification

Using a method and selection criteria very similar to the ones shown in the previous sections, DØ measured the $Z \to \tau\tau$ cross section with a sample of 226 pb^{-1}. The result ($237 \pm 15_{stat} \pm 18_{sys} \pm 15_{lum}$ pb) based on the $Z \to \tau_\mu\tau_{h/e}$ channel [2] is in very good agreement with the Standard Model expectations.

Numerous searches are under way for interesting final states involving taus. Some limits have already been either published, presented at this and other conferences or submitted for publication. Examples include limits on 3rd generation lepto-quark production [3] , R-parity violating SUSY processes [4] or $H \to \tau\tau$ production [5].

9. Conclusions and outlook

The tau identification capabilities of the DØ experiment are now proven. Jet rejections of 99 % or better can be achieved while keeping for taus decaying hadronically or to an electron efficiencies near 70 %. The number of electrons and muons misidentified as taus can be reduced to very low levels. This way, it seems promising that measurements with the tau channels at

DØ can ultimately achieve a few percent precision, making the τ leptons an important handle in the search for new physics at the Tevatron. This wealth of experience will be valuable for all LHC experiments.

REFERENCES

[1] V.M. Abazov et al. (DØ Collaboration), *Nucl. Inst. and Methods Phys. Res. A.* **565**, 463 (2006)

[2] V.M. Abazov et al. (DØ Collaboration), *Phys. Rev. D* **71**, 072004 (2005)

[3] Elemer Nagy, these proceedings

[4] V.M. Abazov et al. (DØ Collaboration), *Phys. Lett. B* **638**, 441 (2006)

[5] V. M. Abazov et al. (DØ Collaboration), *Phys. Rev. Letters* **97**, 121802 (2006)